EURASIP Journal on Applied Signal Processing 2005:3, 397–412

A Low-Cost Time-Hopping Impulse Radio System for High Data Rate Transmission

Andreas F. Molisch ,[1] Ye Geoffrey Li,[2] Yves-Paul Nakache,[1] Philip Orlik,[1] Makoto Miyake,[3] Yunnan Wu,[4] Sinan Gezici,[4] Harry Sheng,[5] S. Y. Kung,[4] H. Kobayashi,[4] H. Vincent Poor,[4] Alexander Haimovich,[5] Jinyun Zhang[1]

[1] *MERL Technology Lab, Mitsubishi Electric Research Laboratories, Cambridge, MA 02139, USA*
Emails: andreas.molisch@ieee.org, nakachey@merl.com, porlik@merl.com, jzhang@merl.com

[2] *School of Electrical and Computer Engineering, Georgia Institute of Technology, Atlanta, GA 30332-0250, USA*
Email: liye@ece.gatech.edu

[3] *Information Technology R&D Center, Mitsubishi Electric Corporation, 5-1-1 Ofuna, Kamakura, Kanagawa 247-8501, Japan*
Email: makoto.miyake@ieee.org

[4] *Department of Electrical Engineering, Princeton University, NJ 08544, USA*
Emails: yunnanwu@princeton.edu, sgezici@princeton.edu, kung@princeton.edu, hisashi@princeton.edu, poor@princeton.edu

[5] *Department of Electrical and Computer Engineering, New Jersey Institute of Technology, Newark, NJ 07102-1982, USA*
Emails: hs23@njit.edu, alexander.m.haimovich@njit.edu

Received 10 October 2003; Revised 1 June 2004

We present an efficient, low-cost implementation of time-hopping impulse radio that fulfills the spectral mask mandated by the FCC and is suitable for high-data-rate, short-range communications. Key features are (i) all-baseband implementation that obviates the need for passband components, (ii) symbol-rate (not chip rate) sampling, A/D conversion, and digital signal processing, (iii) fast acquisition due to novel search algorithms, and (iv) spectral shaping that can be adapted to accommodate different spectrum regulations and interference environments. Computer simulations show that this system can provide 110 Mbps at 7–10 m distance, as well as higher data rates at shorter distances under FCC emissions limits. Due to the spreading concept of time-hopping impulse radio, the system can sustain multiple simultaneous users, and can suppress narrowband interference effectively.

Keywords and phrases: ultra-wideband, impulse radio, RAKE receiver, spectral shaping.

1. INTRODUCTION

Ultra-wideband (UWB) wireless systems are defined as systems that use either a large relative bandwidth (ratio of bandwidth to carrier frequency larger than 25%), or a large absolute bandwidth (larger than 500 MHz). While UWB radar systems have been used for a long time, mainly in the military domain [1], UWB communications systems are a fairly recent development. The first papers in the open literature are those of Win and Scholtz [2, 3, 4], who developed the concept of time-hopping impulse radio (TH-IR) system. This concept excited immense interest in the area of military [5] as well as civilian [6] communications. Further advances of TH-IR are described, for example, in [7, 8, 9, 10, 11]. In 2002, the Federal Communications Commission (FCC) in the US allowed *unlicensed* UWB communications [12]. This greatly increased commercial interest in UWB, leading to a large number of papers (see, e.g., [13, 14]).

One of the most promising applications is data communications at rates that are higher than the currently popular 802.11b (11 Mbps) and 802.11a (< 54 Mbps) standards. The goal, as mandated, for example, by the standardization committee IEEE 802.15.3a, is a system that can provide multiple piconets with 110 Mbps each. This data rate should be achieved for distances up to 10 m (personal area networks). Higher data rates should be feasible at shorter distances.

The principle of using very large bandwidths has several generic advantages.

(i) By spreading the information over a large bandwidth, the spectral *density* of the transmit signal can be made very low. This decreases the probability of intercept

(for military communications), as well as the interference to narrowband victim receivers.

(ii) The spreading over a large bandwidth increases the immunity to narrowband interference and ensures good multiple-access (MA) capabilities [15, 16].

(iii) The fine-time resolution implies high temporal diversity, which can be used to mitigate the detrimental effects of fading [17].

(iv) Propagation conditions can be different for the different frequency components. For example, a wall might be more transparent in a certain frequency range. The large bandwidth increases the chances that at least some frequency components arrive at the receiver [18].

These advantages are inherent in the use of very large bandwidths, and can thus be achieved by *any* UWB system, including the recently proposed UWB frequency-hopping OFDM system [19] and UWB direct-sequence spread spectrum (DS-SS) systems [20]. However, TH-IR has additional advantages.

(i) Recent information-theoretic results indicate that higher capacities can be achieved than with DS-SS systems [21, 22].

(ii) More important from a practical point of view, IR systems operate in baseband only, thus requiring no frequency upconversion circuitry and associated ratio frequency (RF) components [7], though circuitry for accurate timing is still required. This allows low-cost implementation.

A lot of progress has been made in the theoretical understanding of IR, as evidenced by the papers mentioned above. However, several assumptions made in the theoretical analyses do not agree with the requirements for a practical implementation of a high-data-rate IR system. Those requirements may stem from the regulations by the FCC and other frequency regulators, from the necessity of coexistence with other devices, and from cost considerations. The goal of this paper is to describe the complete physical-layer design of an IR system that is suitable for practical implementation. In this system, we combine existing and innovative aspects, paying special attention to the interplay between the different aspects. The current paper is thus more of an "engineering" paper, while the theoretical background of some of our innovations is described in [23, 24, 25].

The rest of the paper is organized in the following way. In Section 2, we present an overview of the system. Next, we discuss the transmit signal, and how its spectrum can be shaped to fit the requirements of regulators, as well as to minimize interference to nearby devices. Section 4 describes the signal detection at the receiver, including the structure of the RAKE receiver and the equalizer. The channel estimation procedure that is used for establishing the weights of the RAKE receiver and equalizer is discussed in Section 5. Finally, Section 6 presents simulations of the total performance of the system in terms of coverage and resistance to interference from narrowband signals and other UWB transmitters. A summary and conclusions wrap up the paper.

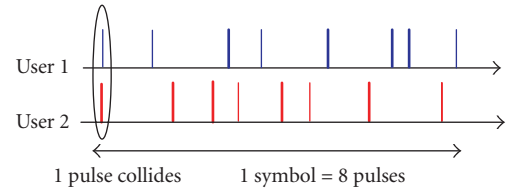

Figure 1: Principle of TH-IR for the suppression of catastrophic collisions.

2. SYSTEM OVERVIEW

The system that we are considering is a TH-IR system. We first describe "classical" TH-IR [4]. Each data bit is represented by several short pulses; the duration of the pulses essentially determines the bandwidth of the (spread) system. For the single-user case, it would be sufficient to transmit a single pulse per symbol. However, in order to achieve good MA properties, we have to transmit a whole sequence of pulses. Since the UWB transceivers are unsynchronized, so-called "catastrophic collisions" can occur, where pulses from several transmitters arrive at the receiver, almost simultaneously. If only a single pulse would represent one symbol, this would lead to a bad signal-to-interference ratio (SIR), and thus to a high bit error probability BER. These catastrophic collisions are avoided by sending a whole sequence of pulses instead of a single pulse. The transmitted pulse sequence is different for each user, according to a so-called TH code. Thus, even if one pulse within a symbol collides with a signal component from another user, other pulses in the sequence will not. This achieves an interference suppression gain that is equal to the number of pulses in the system. Figure 1 shows the operating principle of a generic TH-IR system. We see that the possible positions of the pulses within a symbol follow certain rules: the symbol duration is subdivided into N_f "frames" of equal length. Within each frame, the pulse can occupy an almost arbitrary position (determined by the TH code). Typically, the frame is subdivided into "chips," whose length is equal to a pulse duration. The (digital) TH code now determines which of the possible positions the pulse actually occupies. The modulation of this sequence of pulses can be pulse-position modulation (PPM), as suggested in [4], or pulse-amplitude modulation (PAM). PPM has the advantage that the detector can be simpler (an energy detector) in AWGN channels. However, reception in multipath environments requires a RAKE receiver for either PPM or PAM.

While this scheme shows good performance for some applications, it does have problems for high-data-rate, FCC-compliant systems.

(1) Due to the use of PPM, the transmit spectrum shows spectral lines. This requires the reduction of the total emission power, in order to allow the fulfillment of the FCC mask within each 1 MHz band, as required by the FCC.

(2) Due to the high data rate required by 802.15, and due to the high delay spread seen by indoor channels, the system works better with an equalizer. An equalizer for

PPM will introduce increased complexity and cost.

(3) For a full recovery of all considered multipath components (MPCs), the system requires a RAKE receiver with a large number of fingers. A conventional implementation, using many digital correlators, will also introduce increased complexity and cost.

(4) Due to the relatively low spreading factor of less than 40, the number of possible pulse positions within a frame is limited. This might lead to a higher collision probability, and thus smaller interference suppression.

The first two problems are solved by using (antipodal) PAM instead of PPM. This eliminates the spectral lines, and allows, in general, an easier shaping of the spectrum. Furthermore, it allows the use of simple linear equalizers. As detailed below, an innovative RAKE receiver is considered to overcome the third problem; this RAKE structure implements correlators by means of pulse generators and multipliers only. The problem of MA interference, finally, can be addressed by interference-suppressing combining of the RAKE-finger signals.

A block diagram of the system is shown in Figure 2. The transmit data stream is divided into blocks, and each block is encoded with a convolutional coder. We use a rate 1/2 convolutional code with a constraint length 7. The use of turbo codes or low-density parity check codes would improve the performance by approximately 2 dB; however, decoding becomes challenging at the high data rates envisioned in this scheme. Then, a preamble is prepended that can be used for both acquisition and channel estimation. As mentioned above, the modulation and MA format is a BPSK-modulated TH-IR. Each pulse sequence representing one symbol is multiplied by ± 1, depending on the bit to be transmitted. Finally, each data block (including preamble) is amplified (with power control, in order to minimize interference to other systems) and transmitted. Note that as the system is packet based and the number of packets per second can vary, it is not desirable to code across packets.

In the receiver, the acquisition part of the preamble is stripped off and used to determine the timing. Once this has been established, the "channel estimation part" of the preamble is used to determine the coefficients for the RAKE receiver and the equalizer. The main body of the data block is then received by a RAKE receiver that can be interpreted as a filter that is matched to the convolution of the transmit signal and the channel impulse response. Each finger of the RAKE is a filter that is matched to a time-delayed version of the transmit signal, encompassing both the pulse shape and the TH sequence. We use here an innovative RAKE structure that requires only pulse generators and no delays, which makes an analog implementation possible—this allows us to perform the sampling and A/D conversion only at the *symbol rate* instead of the chip rate. Note that for chip-rate sampling, analog-to-digital (A/D) converters with about 20 Gsamples/s would be required. The outputs of the RAKE fingers are weighted (according to the principles of optimum combining) and summed up. The optimum location and weight of the fingers can be determined from the channel sounding sequence, which is processed before the reception of the actual data. The output of the summer is then sent through a minimum mean square error (MMSE) equalizer and a decoder for the convolutional code.

One important point of the system is that all the pulses are *baseband* pulses, more specifically, derivatives of Gaussian pulses. This allows a simple pulse generation, and obviates any need for passband components. This is a typical property of TH-IR; however, it is not a trivial task within the restrictions of the FCC that the main power is emitted in the 3–10 GHz range. We will show in Section 3 how this can be achieved.

The goal of our design is to obtain a low-cost implementation. Thus, the design is not theoretically optimum, but rather contains a number of simplifications that reduce complexity of implementation and costs.

3. TRANSMIT WAVEFORM AND SPECTRAL SHAPING

3.1. Mathematical description of the transmit waveform

Throughout this paper, we use a communication system model, where the transmit signal is given by

$$\begin{aligned} s_{\mathrm{tr}}(t) &= \sum_{j=-\infty}^{\infty} d_j b_{\lfloor j/N_f \rfloor} w_{\mathrm{tr}}(t - jT_f - c_j T_c) \\ &= \sum_{k=-\infty}^{\infty} b_k w_{\mathrm{seq}}(t - kT_s), \end{aligned} \tag{1}$$

where $w_{\mathrm{tr}}(t)$ is the transmitted unit-energy pulse, T_f is the average pulse repetition time, N_f is the number of frames (and therefore also the number of pulses) representing one information symbol of length T_s, and b is the transmitted information symbol, that is, ± 1; $w_{\mathrm{seq}}(t)$ is the transmitted pulse sequence representing one symbol and $\lfloor x \rfloor$ denotes the smallest integer than x. The TH sequence provides an additional time shift of $c_j T_c$ seconds to the jth pulse of the signal, where T_c is the chip interval, and c_j are the elements of a pseudorandom sequence, taking on integer values between 0 and $N_c - 1$. To prevent pulses from overlapping, the chip interval is selected to satisfy $T_c \leq T_f/N_c$; in the following, we assume $T_f/T_c = N_c$ so that N_c is the number of chips per frame. We also allow "polarity scrambling" (see Section 3.4), where each pulse is multiplied by a (pseudo-) random variable d_j that can take on the values $+1$ or -1, with equal probability. The sequence d_j is assumed to be known at the transmitter and the receiver.

An alternative representation can be obtained by defining a sequence $\{s_j\}$ as follows:

$$s_j = \begin{cases} d_{\lfloor j/N_c \rfloor} & \text{for } j - N_c \left\lfloor \dfrac{j}{N_c} \right\rfloor = c_{\lfloor j/N_c \rfloor}, \\ 0 & \text{otherwise.} \end{cases} \tag{2}$$

Then the transmit signal can be expressed as

$$s_{\mathrm{tr}}(t) = \sum_{j=-\infty}^{\infty} s_j b_{\lfloor j/N_f N_c \rfloor} w_{\mathrm{tr}}(t - jT_c). \tag{3}$$

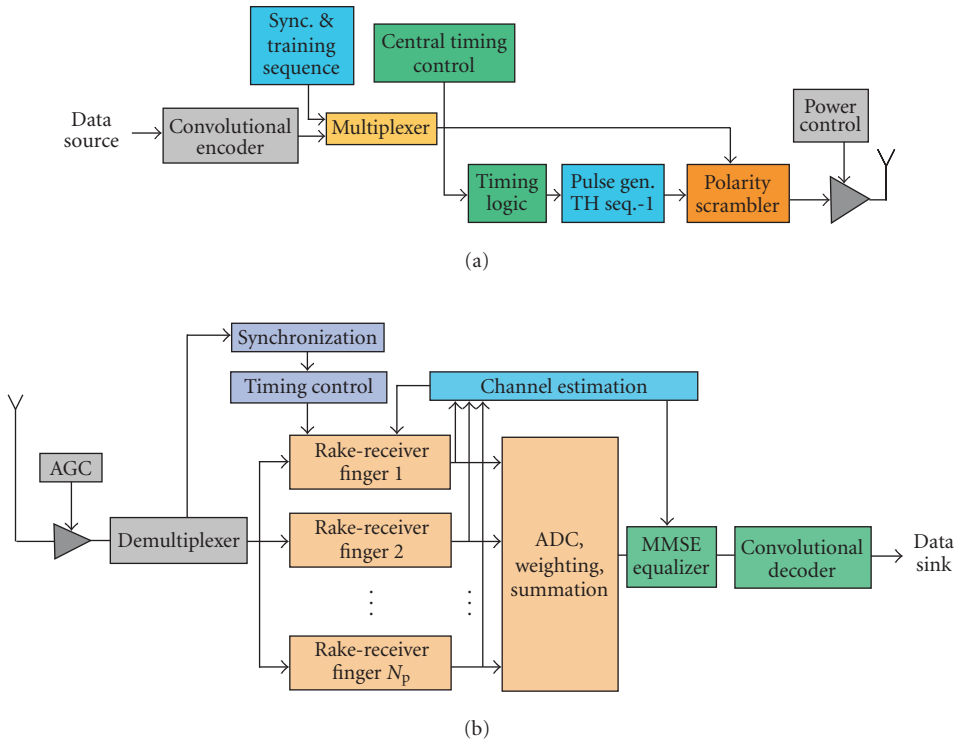

Figure 2: Block diagram of (a) the transmitter and (b) the receiver.

To satisfy the spectrum masking requirement of the FCC, the transmit waveform w_{tr}, also known as monocycle waveform, is chosen to be the fifth derivative of the Gaussian pulse and it can be expressed as

$$w_{\text{tr}}(t) = p(t) = K_2\left(-15\frac{t}{\sigma_p} + 10\frac{t^3}{\sigma_p^3} - \frac{t^5}{\sigma_p^5}\right)\exp\left(-\frac{t^2}{2\sigma_p^2}\right), \tag{4}$$

where K_2 is a normalization constant, and σ_p controls the width of the pulse and it is chosen according to the spectral mask requirement of the FCC, as [26]

$$\sigma_p = 5.08 \times 10^{-11}\,\text{s}. \tag{5}$$

Other signals shapes are possible; in particular, a combination of weighted pulses $p(t)$ (as explained below) can be used to improve the spectral properties. The various methods (e.g., RAKE receiver, pulse-polarity randomization, etc.) discussed in the rest of the paper can be applied independently on the exact shape of the transmit waveform.

3.2. Spectral shaping—general aspects

One of the key requirements for a UWB system is the fulfillment of the emission mask mandated by the national spectrum regulators [27]. In the USA, this mask has been prescribed by the FCC and essentially allows emissions in the 3.1–10.6 GHz range with power spectral density of −41.3 dBm/MHz; in Europe and Japan, it is still under discussion. In addition, emissions in certain parts of the band (especially the 5.2–5.8 GHz range used by wireless LANs) should be kept low, as UWB transceivers and IEEE 802.11a transceivers, which operate in the 5 GHz range, are expected to work in close proximity. We are using two techniques in order to fulfill those requirements.

(i) The first is a linear combination of a set of basis pulses to be used for shaping of the spectrum of a transmitted IR signal. The delayed pulses are obtained from several appropriately timed programmable pulse generators. The computation of the delays and weights of those pulses is obtained in a two-step optimization procedure [23].

(ii) A further improvement of the spectral properties can be obtained by exploiting different polarities of the pulses that constitute a transmit sequence $w_{\text{seq}}(t)$. Using different pulse polarities does not change anything for signal detection, as it is known at the receiver, and can thus be easily reversed. However, it does change the spectrum of the *emitted* signal, and thus allows a better matching to the desired frequency mask [24, 28].

The first technique (combination of pulses) leads to a shaping of the spectrum, allowing the placement of broad minima and an efficient "filling out" of the FCC mask.

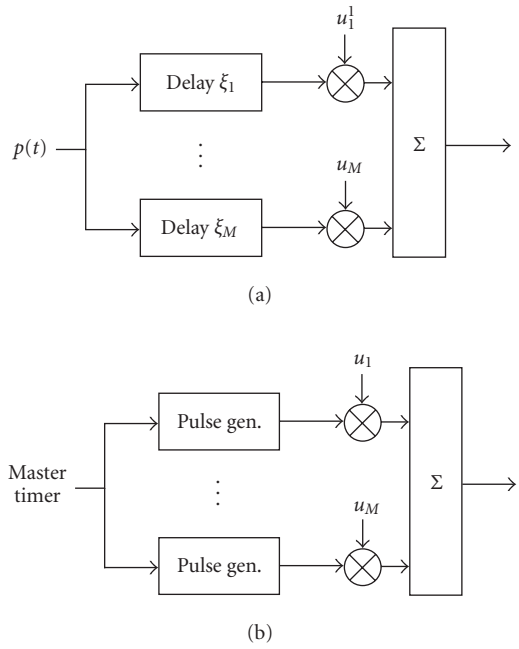

FIGURE 3: Principle of pulse combination for spectral shaping with (a) delay lines and with (b) programmable pulse generators.

The second technique is used to reduce or eliminate the peak-to-average ratio of the spectrum, and allows the design of more efficient MA codes. Note that these two aspects are interrelated, and the optimization of pulse combination and polarity randomization should be done jointly in order to achieve optimality. However, such a joint treatment is usually too complicated for adaptive modifications of the transmit spectrum.

A further important aspect of the spectral shaping is that it can be used not only to reduce interference *to* other devices, but also interference *from* narrowband interferers. This can be immediately seen from the fact that matched filtering is used in the receiver. Placing a null in the transmit spectrum thus also means that the receiver suppresses this frequency. Furthermore, it might be advantageous in some cases to perform "mismatched filtering" at the receiver by placing minima in the receive-transfer function even if there is no corresponding minimum in the transmit spectrum. This is useful especially for the suppression of narrowband interferers that could otherwise drive the A/D converter into saturation.

3.3. Pulse combination

One of the key problems of "conventional" TH-IR radio is that it is difficult to influence its spectrum without the use of RF components. Spectral notches, for example, are typically realized by means of band-block filters. However, this is undesirable for low-cost applications; furthermore, it does not allow adaptation to specific interference situations. We have thus devised a new scheme for shaping the spectrum [23]. This scheme uses delaying and weighting of a set of basis pulses to influence the transmit spectrum, (see Figure 3).

The basic transmit waveform $w_{\mathrm{tr}}(t)$ is a sum of delayed and weighted "basic pulse shapes" $p(t)$ that can be easily generated, for example, Gaussian pulses and their derivatives:

$$\begin{aligned} w_{\mathrm{tr}}(t) &\equiv \sum_{i=0}^{M} u_i p(t-\xi_i), \\ W(\mathrm{j}\Omega) &\equiv \int_{-\infty}^{\infty} w_{\mathrm{tr}}(t) e^{-j\Omega t} dt = \sum_{i=0}^{M} u_i P(j\Omega) e^{-j\Omega\xi_i}, \end{aligned} \tag{6}$$

where j is the imaginary unit (not to be confused with the index j that denotes the considered frame), u_i are the pulse weights, $W(\mathrm{j}\Omega)$ is the Fourier transform of $w_{\mathrm{tr}}(t)$, and Ω is the transform variable. In contrast to tapped delay lines, where only certain discrete delays are feasible, we assume here that a continuum of delays can be chosen. This can be achieved by the use of programmable pulse generators. The range of allowed delays of the coefficients is determined by the pulse-repetition frequency of the communication system. The number of pulse generators $M+1$ should be kept as low as possible to reduce the implementation costs.

We introduce the following notations:

$$\begin{aligned} \underline{u} &\equiv \begin{bmatrix} u_0 & u_1 & \cdots & u_M \end{bmatrix}^{\mathrm{T}}, \\ \underline{\xi} &\equiv \begin{bmatrix} \xi_0 & \xi_1 & \cdots & \xi_M \end{bmatrix}^{\mathrm{T}}, \\ r(\lambda) &\equiv \int_{-\infty}^{\infty} p(t-\lambda) p(t) dt = r(-\lambda), \\ \mathbf{R}(\underline{\xi}) &\equiv \begin{pmatrix} r(0) & r(\xi_0-\xi_1) & \cdots & r(\xi_0-\xi_M) \\ r(\xi_1-\xi_0) & r(0) & \ddots & r(\xi_1-\xi_M) \\ \vdots & \ddots & \ddots & \vdots \\ r(\xi_M-\xi_0) & r(\xi_M-\xi_1) & \cdots & r(0) \end{pmatrix}, \\ \langle w_{\mathrm{tr}}(t), w_{\mathrm{tr}}(t) \rangle &\equiv \int_{-\infty}^{\infty} w_{\mathrm{tr}}(t) w_{\mathrm{tr}}(t) dt = \underline{u}^{\mathrm{T}} \mathbf{R}(\underline{\xi}) \underline{u}. \end{aligned} \tag{7}$$

The single-user spectrum shaping problem can now be formulated as follows:

$$\max_{\underline{u},\underline{\xi}} \langle w_{\mathrm{tr}}(t), w_{\mathrm{tr}}(t) \rangle, \quad \text{subject to } |W(j\Omega)|^2 \le M(\Omega), \quad \forall \Omega \in [-\infty, \infty], \tag{8}$$

where $M(\Omega)$ is the upper bound on the magnitude response regulated by FCC. This is equivalent to

$$\min_{\underline{u},\underline{\xi}} \max_{\Omega \in [-\infty,\infty]} \frac{|W(j\Omega)|^2}{M(\Omega)}, \quad \text{subject to } \underline{u}^{\mathrm{H}} \mathbf{R}(\underline{\xi}) \underline{u} = 1. \tag{9}$$

The criteria for the optimization $M(\Omega)$ can thus stem from the FCC spectral mask, which is fixed, from the necessity to avoid interference to other users, which can be predefined or time varying, or following an instantaneous or averaged determination of the emissions of users in the current environment, or other criteria. In any case, these criteria are mapped onto an "instantaneous" spectral mask that has to

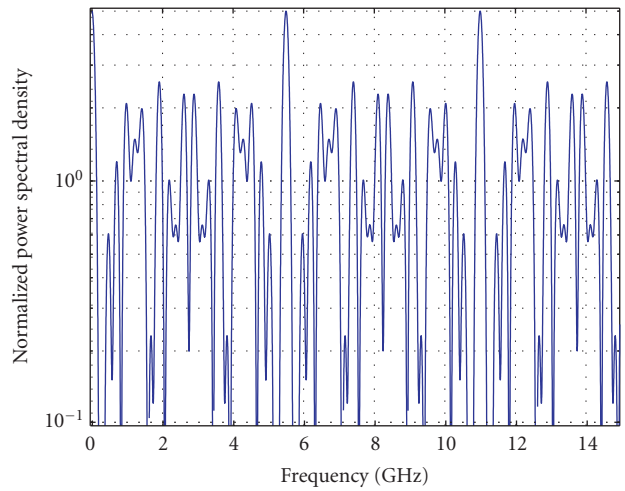

Figure 4: Spectrum of TH sequence with "classical" impulse radio: 5 chips each in 5 frames. Positions of the pulses are given by the chip sequence [1 0 0 0 0 0 0 0 1 0 0 0 1 0 0 0 0 1 0 0 0 0 0 1 0].

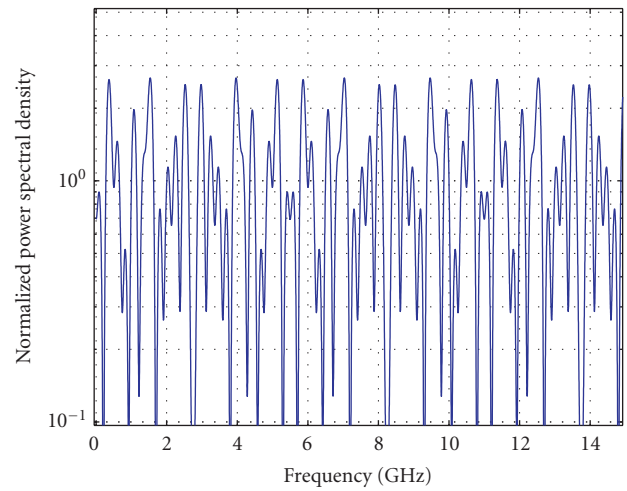

Figure 5: Spectrum of the PAM signal with polarity randomization of the TH sequence using the same positions of the pulses as in Figure 4, with normalized pulse amplitudes given by the weighting vector $[-0.5 \;\; 0.5 \;\; 0.5 \;\; -0.5 \;\; 1.5]$.

be satisfied by the pulse. If the fulfillment of the FCC spectral mask is the only requirement, then the optimum weights can be computed a priori, and stored in the transceivers; in that case, the computation time determining the optimum weights and delays is not relevant, and exhaustive search can be used. However, in order to adjust to different interference environments, a capability to optimize the weights dynamically is desirable. This can be achieved, for example, by an efficient two-step procedure that in the first step uses an *approximate* formulation of the optimization problem, namely two-norm minimization that can be solved in closed form. This solution is then used as the initialization of a nonlinear optimization (e.g., by means of a neural network) to find the solution to the *exact* formulation. Details of this two-step procedure can be found in [23]. Note also that the spectral shaping can be refined even more by combining different basis pulses. However, this requires different pulse generators, which increases implementation complexity.

3.4. Polarity randomization

Conventional IR systems use only a pseudo-random variation of the pulse position to distinguish between different users. For PAM-TH-IR, the spectrum of the transmit signal is determined by the spectrum of the transmit waveform $w_{\text{tr}}(t)$ multiplied with the spectrum of the TH sequence. Figure 4 shows an example of a spectrum with a short (5 frames) TH sequence, in combination with a fifth-order Gaussian basis pulse. We can observe strong ripples, so that the peak-to-average ratio is about 6 dB. However, the ideal case would be to find TH sequences whose spectrum is flat, so that the we can design the transmit waveform to fit the spectral mask as closely as possible. One way to achieve this goal is to use very long TH sequences (much longer than a symbol duration). However, this complicates the design of the receiver, especially the equalizer. Alternatively, we can use more degrees of freedom in the design of short sequences by allowing different amplitudes and polarities of the pulses for the design of the sequence. This helps to limit the power backoff by reducing the peak-to-average ratio. However, it is still true that the less pulses that compose the sequence, the larger is the peak-to-average ratio. An example can be seen by comparing Figure 5 (polarity randomization) to Figure 4 (unipolar sequence); it is obvious that the ripples have been considerably reduced; specifically, we reduced the peak-to-average ratio by 1.6 dB. We also have to bear in mind that we need to generate a multitude of sequences that all should have the desired spectral properties, as well as approximate orthogonality with respect to each other for arbitrary time shifts of the sequences. This is a complex optimization problem, and has to be solved by an exhaustive search.

4. SIGNAL DETECTION

4.1. Received signal and RAKE reception

The RAKE receiver is a key aspect of UWB systems.[1] Due to the ultra-wide bandwidth, UWB systems have very fine temporal resolution, and are thus capable of resolving MPCs that are spaced approximately at an inverse of the bandwidth. This is usually seen as a big advantage of UWB. Multipath resolution of components reduces signal fading because the MPCs undergo different fading, and thus represent different diversity paths. The probability that all the components are simultaneously in a deep fade is very low. However, the fine time resolution also means that many of the MPCs have to be "collected" by the RAKE receiver in order to obtain all of the available energy. A channel with N_{p} resolvable paths requires

[1] An exception is OFDM-based UWB systems, which use a different principle to collect the multipath energy [19].

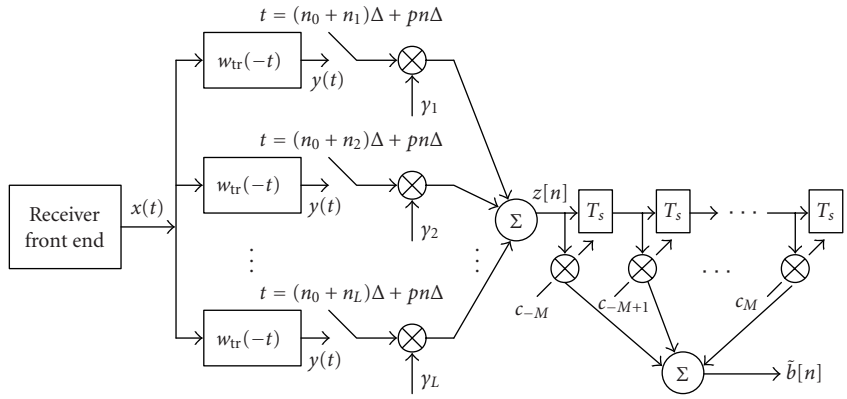

Figure 6: Structure of RAKE receiver and equalizer.

N_p fingers to collect all of the available energy. In a dense multipath environment, the number of MPCs increases linearly with the bandwidth. Even a sparse environment, such as specified by the IEEE 802.15.3a standard channel model [29], requires up to 80 fingers to collect 80% of the available energy.

Another problem is the complexity of the RAKE fingers. In the conventional RAKE finger of a DS-SS system, the received signal is filtered with a filter matched to the chip waveform, and then in each RAKE finger, correlated to time-shifted versions of the spreading sequence. In order to do the correlation, the signal first has to be sampled and A/D converted at the chip rate. Then, those samples have to be processed. This involves convolution with the stored reference waveform, addition, and readout. Sampling and A/D converting at the chip rate, for example, 10 Gsamples/s, requires expensive components.[2]

We avoid those problems by utilizing a RAKE/equalizer structure as outlined in Figure 6. Each RAKE finger includes a programmable pulse generator, controlled by a pulse sequence controller. The signal from the pulse generator is multiplied with the received signal. The output of the multiplier is then sent through a low-pass filter, which generates an output proportional to a time integral of an input to the filter. The implementation is analog, while the adjustable delay blocks have been eliminated. The hardware requirements for each RAKE finger are one pulse generator (which can be controlled by the same timing controller), one multiplier, and one sampler/AD converter. It is an important feature of this structure that the sampling occurs at the *symbol* rate, not the chip rate. In the following, we assume the use of 10 RAKE fingers; this is a very conservative number. Obviously, a larger number of RAKE fingers would give better performance; this is one of the complexity/performance tradeoffs in our design [30, 31]. The weights for the combination of the fingers are determined by the channel estimation procedure described in Section 5.

[2]Note that some companies have proposed the use of *one-bit* A/D converters with 7.5–20 Gsamples per second [20].

Next, we compute the output of the different RAKE fingers. Let the impulse response of a UWB channel be

$$h(t) = \sum_k \alpha_k \delta(t - \tau_k), \tag{10}$$

where τ_k and α_k are the delay and (real) gain of the kth path of the UWB channel, respectively. Then the channel output can be expressed as

$$x(t) = h(t) * s_{\text{tr}}(t) + \overline{n}(t) = \sum_{n=-\infty}^{\infty} b_n \hat{h}(t - nT_s) + \overline{n}(t), \tag{11}$$

where

$$\hat{h}(t) = \sum_k \alpha_k w_{\text{tr}}(t - \tau_k). \tag{12}$$

The output of the matched filter can be expressed as

$$y(t) = x(t) * w_{\text{tr}}(-t) = \sum_{k=-\infty}^{\infty} b_k \tilde{h}(t - kT_s) + \tilde{n}(t), \tag{13}$$

where

$$\begin{aligned} \tilde{h}(t) &= \int \hat{h}(t - \tau) w_{\text{tr}}(-\tau) d\tau = \sum_k \alpha_k r(t - \tau_k), \\ r(t) &= \int w_{\text{tr}}(t + \tau) w_{\text{tr}}(\tau) d\tau, \\ \tilde{n}(t) &= \overline{n}(t) * w_{\text{tr}}(-t). \end{aligned} \tag{14}$$

The samples of the matched filter output can be thus written as

$$y[n] = y(n\Delta) = \sum_{k=-\infty}^{\infty} b_k \tilde{h}(n\Delta - kp\Delta) + \tilde{n}(n\Delta), \tag{15}$$

where Δ is the minimum time difference between RAKE fingers and $p = T_s/\Delta$.

4.2. Combining of the Rake signals

Let $\tilde{h}(n_l\Delta)$'s, for $l = 1, \ldots, L$, be the L taps with the largest absolute values $|\tilde{h}(n_l\Delta)|$'s. The output of the RAKE receiver can be expressed as

$$z[n, n_o] = \sum_{l=1}^{L} \gamma_l y[pn + n_l + n_o], \tag{16}$$

where γ_l is the weight for the lth finger and n_o is a time offset. It is obvious that the signal quality of the RAKE receiver's output depends on the weight and initial time offset.

Maximal ratio combining (MRC) is a traditional approach to determine the weights of the RAKE combiner. For the MRC RAKE combiner, $\gamma_l = \tilde{h}(n_l\Delta)$ and

$$z[n, n_o] = \sum_{l=1}^{L} \tilde{h}(n_l\Delta)\, y[pn + n_l + n_o]. \tag{17}$$

MMSE RAKE combining can improve the performance of the RAKE receiver in the presence of interference, including intersymbol interference (ISI) and multiuser interference, since it automatically take the correlation of the interference into consideration. For the MMSE RAKE combiner, the weights are determined to minimize

$$E\left\{ |z[n, n_o] - b_n|^2 \right\}. \tag{18}$$

The performance of the RAKE receiver can be further improved if *adaptive timing* is used with the MMSE RAKE combiner. That is, the goal is to find optimum time offset n_o and γ_l to minimize (18).

When there is cochannel interference, the received signal can be written as

$$\bar{y}[n] = \sum_{k=-\infty}^{\infty} b_k \tilde{h}(n\Delta - kT_s) + \underbrace{\sum_{k=-\infty}^{\infty} \bar{b}_k \bar{h}(n\Delta - kT_s) + \tilde{n}(n\Delta)}_{i[n]}, \tag{19}$$

where $\{\bar{b}_k\}$ and $\bar{h}(n\Delta - kT_s)$ are, respectively, i.i.d. sequence and channel impulse response corresponding to the interferer, and $i[n]$ represents the interference-plus-noise. It can be shown that $i[n]$ is not stationary but rather cyclostationary. Let

$$P_k = E\left\{ |i[mp + k]|^2 \right\}, \tag{20}$$

for any integer m and $k = 0, 1, \ldots, p-1$. Therefore, for different k, $h(nT_s + k\Delta)$ experiences different interference power. To improve the performance of the RAKE receiver, we need to normalize the channel impulse response corresponding to the desired signal by

$$\hat{h}(n\Delta) = \frac{\tilde{h}(n\Delta)}{\sqrt{P_k}}, \tag{21}$$

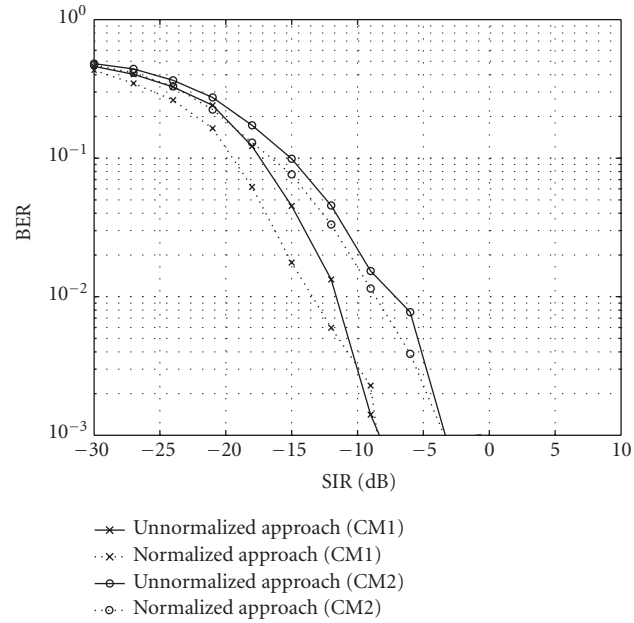

Figure 7: Interference suppression performance for one interferer and SNR = 50 dB.

and then find the L taps with the largest absolute values of channel taps $|\hat{h}(n_l\Delta)|$'s for the RAKE receiver.

Figure 7 demonstrates the interference suppression performance for a UWB system with one interferer and 50 dB signal-to-noise ratio (SNR). We compare the BER without normalization to the improved one that is normalized by noise power as described above. Note that this can also be interpreted as the difference between assuming the interference being stationary or cyclo-stationary.

4.3. Channel equalizer

The combination of the channel and the RAKE receiver constitutes an equivalent channel; however, since the symbol duration is shorter than the delay spread of the channel, ISI does occur. We combat that by means of an MMSE equalizer, as indicated in Figure 6. The reasons for choosing a linear equalizer, instead of a decision-feedback equalizer (DFE), are twofold.

(i) The system is intended to operate at symbol error probabilities of 1–10%; strong coding is used to decrease the frame error probability. Thus, a decision feedback of the "raw symbols" (hard decision before the decoder) would result in strong error propagation.

(ii) The alternative to use the symbols after decision would require reencoding and remodulation before subtraction. This increases complexity considerably. As the ISI is not a dominant source of errors in our system (as determined from simulations that are not described in detail in Section 6), the possible gains from this improved DFE scheme do not warrant such an increase in complexity.

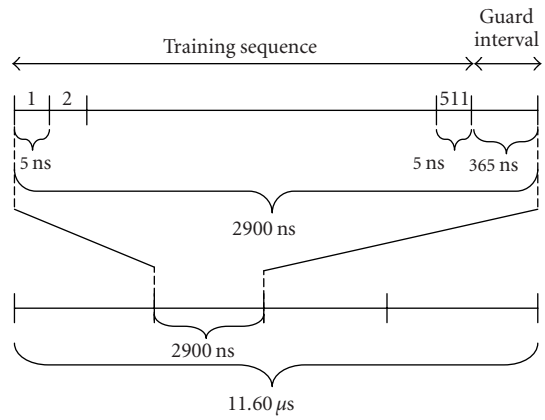

Figure 8: Structure of the training sequence.

After the RAKE receiver, a linear equalizer is used to mitigate residual interference. Let the coefficients of the equalizer be $\{c_{-K}, c_{-K+1}, \ldots, c_{-1}, c_0, c_1, \ldots, c_K\}$. Then the equalizer output is

$$\tilde{b}[n] = \sum_{k=-K}^{K} c_k z[n-k, n_o]. \tag{22}$$

To optimize performance, the equalizer coefficients are chosen to minimize the MSE of its output, that is,

$$\text{MSE} = E\left\{ \left| \tilde{b}[n] - b_n \right|^2 \right\}. \tag{23}$$

For the numerical simulations in Section 6, we will use a five-tap equalizer.

5. PARAMETER ESTIMATION

A training sequence is used to determine the parameters for the RAKE receivers and equalizers. It is desirable to use the correlators and A/D converters of the RAKE receivers, since these components have to be available anyway. This is not straightforward, as the sampling and A/D conversion of the correlator outputs is done at the symbol rate, while the channel parameters have to be available for each possible chip-sampling instant. This problem is solved by combining a "sliding correlator" approach with a training sequence that exhibits a special structure, as shown in Figure 8.

5.1. Channel estimation

The matched filter in the RAKE receiver in UWB systems is implemented using analog circuits since it needs to operate at a high speed. The output of the matched filter is sampled at symbol rate ($1/T_s = 1/(p\Delta)$). Therefore, during each symbol period, we can only observe L outputs, one form each of the L fingers. On the other hand, we need to estimate channel coefficients every Δ seconds; thus we need to obtain p uniform samples during each symbol period.

In order to solve this seeming paradox, we use an approach that shows some similarity to the "swept time-delay cross-correlator" channel sounder proposed in [32]. We send the same training sequence (with guard interval) multiple times to obtain denser sampling of the matched filter output. For a RAKE receiver with 10 fingers, 10 samples with different timings can be obtained within one symbol duration if the training sequence is sent once. Therefore, to get 32 samples per symbol duration, the training sequence needs to be repeated 4 times (see also Figure 8). Each training sequence consists of 511 symbols, and 365 nanoseconds guard interval to prevent interference caused by delay spread of UWB channels between adjacent training sequences. Consequently, the length of the whole training period for parameter estimation is $4(511 * 5 + 365) = 11600$ nanoseconds or 11.6 microseconds. The detailed equations for the channel estimates can be found in the appendix.

Figures 9 and 10 show the normalized MSE (NMSE) of our channel estimation, which is defined as

$$\text{NMSE} = \frac{\sum_n \left| \tilde{h}(n\Delta) - h(n\Delta) \right|^2}{\sum_n \left| h(n\Delta) \right|^2}. \tag{24}$$

From Figure 9, the channel estimation improves with the SNR when it is less than 35 dB. However, when it is over 35 dB, there is an error floor. Figure 10 shows the NMSE of the 10 largest channel taps, which is much better than the NMSE of the overall channel estimation.

After having obtained the channel estimates, we determine the optimum RAKE combining weights by minimizing the mean square error (MSE). The concatenation of the channel and the RAKE receiver constitutes a "composite" channel that is sampled once per symbol. The equalizer is adapted such that it minimizes the MSE of the equalizer output compared to a special training sequence that is transmitted after the RAKE weights have been adjusted. Detailed equations about the weights for RAKE and equalizer can be found in the appendix.

5.2. Synchronization

Before any data demodulation can be done on the received UWB signal, the template signal and the received signal must be time-aligned. The aim of acquisition is to determine the relative delay of the received signal with respect to the template signal. The conventional technique to achieve this is the serial-search algorithm. In this scheme, the received signal is correlated with a template signal and the output is compared to a threshold. If the output is lower than the threshold, the template signal is shifted by some amount, which usually is comparable to the resolvable path interval, and the correlation with the received signal is obtained again. In this way, the search continues until an output exceeds the threshold. If the output of the correlation comes from a case where signal paths and the template signal are aligned, it is called a signal-cell output. Otherwise, it is called a nonsignal-cell output. A false alarm occurs when a nonsignal-cell output exceeds the threshold. In this case, time t_p elapses until the search recovers again. This time is called penalty time for false alarm.

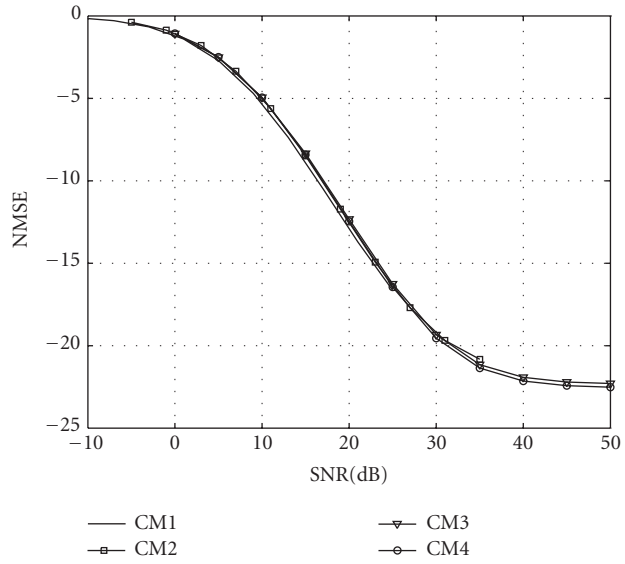

Figure 9: NMSE of the overall channel estimation in IEEE 802.15.3a channel models (see Section 6).

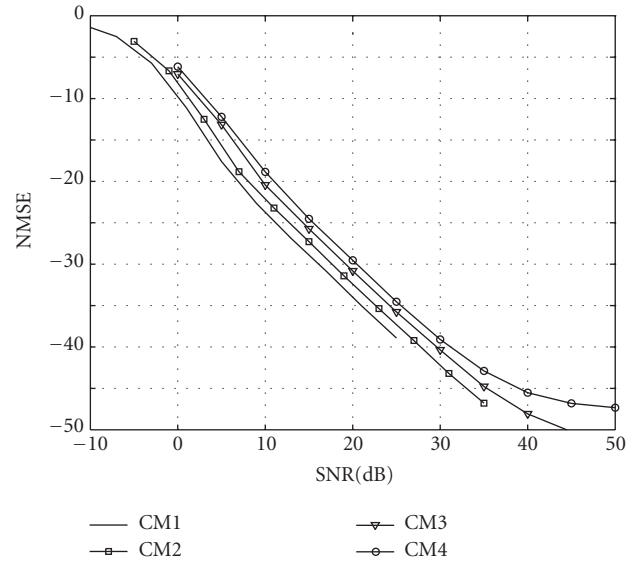

Figure 10: NMSE of the 10 largest channel taps in IEEE 802.15.3a channel models (see Section 6).

However, in UWB systems, such a sequential search can be very time consuming, as the number of cells is very large. This problem can be overcome by a new algorithm that we call "sequential block search." The key idea here is to divide the possible search space, which contains the cells, into several blocks, where each of the blocks contains a number of signal cells. We then first perform a quick test to check if the whole block contains a signal cell or not. Once we have identified the block that contains the signal, a more detailed (sequential) search is performed in that block; for details, see [25]. Simulations show that acquisition can be achieved (with 90% probability) in less than 10 microseconds. This can be shortened even further if the search space is restricted, for example, by exploiting knowledge [3] from a beacon signal.

6. PERFORMANCE RESULTS

In this section, we analyze the performance of our system in multipath and interference. The performance of the system was simulated in "typical" UWB channels, which were developed within the IEEE 802.15.3a UWB standardization activities and are described in detail in [29]. We distinguish between four different types of channels (called CM1, CM2, CM3, and CM4). CM1 describes line-of-sight (LOS) scenarios with distances between the transmitter and the receiver of less than 4 m; CM2 and CM3 describe non-LOS scenarios at distances 0–4, and 4–10 m, respectively. CM4 is valid for heavy multipath environments. Note that in the following, we will plot the performance in all the four different types of channels over a wide range of distances.[4]

Figure 11 shows the probability for obtaining a successful link. A "successful" link means that acquisition is obtained successfully, and the packet error probability (over the ensemble of different channels) is less than 8%. For CM1, the mean coverage distance is about 10 m. The 10% outage distance (meaning that 8% of the packet error rate (PER) or less is guaranteed in 90% of all channels) is 7 m.[5] For heavy multipath (CM4), these values decrease to 7 and 4 m, respectively.

Figure 12 shows the analogous curves for a data rate of 200 Mbps. Due to the higher rate, the original data stream is converted (demultiplexed) into two parallel data streams with 100 Mbps each. The two data streams are then transmitted simultaneously, using TH codes that have the same hopping sequence, but are offset in delay by one chip. In an AWGN channel, those codes would remain orthogonal, and the performance should be worsened only by 3 dB (since the E_b/N_0 is decreased). However, in a multipath channel, the temporally offset codes lose their orthogonality, which worsens the performance. One way to remedy this situation is to use different (not just offset) hopping codes. However, this decreases the number of possible simultaneous piconets. Another approach would be the use of the scheme

[3] Note that the threshold whether detection has taken place or not is a critical parameter of the algorithm. A discussion of how to set this threshold can be found in [25].

[4] We also evaluate the performance at distances that the IEEE models were not originally intended for (e.g., CM1 was extracted from measurements where the distance between the transmitter and the receiver is less than 4 m). We do this as it gives insights into the relative importance of delay dispersion and attenuation.

[5] The mean coverage distance is defined as the distance where the packet error rate, averaged over all channel realizations, is below the target rate (PER).

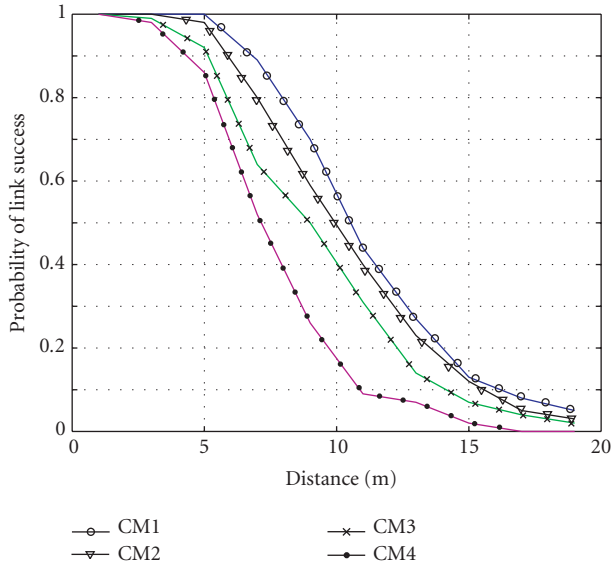

Figure 11: Probability of link success as a function of distance for 110 Mbps mode.

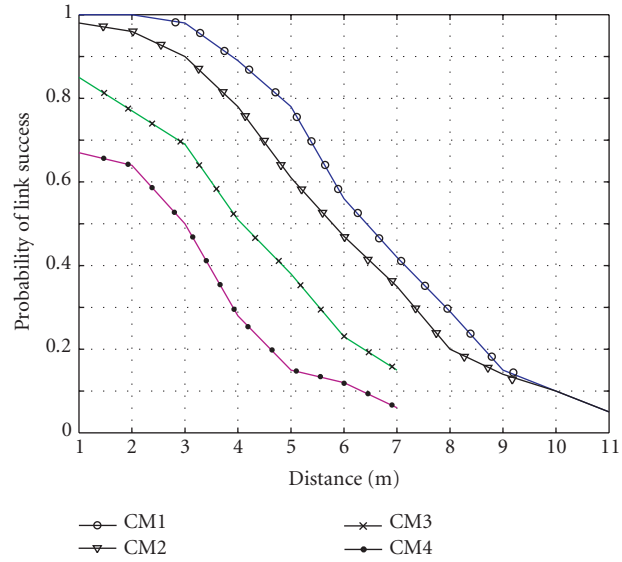

Figure 12: Probability of link success as a function of distance for the 200 Mbps mode.

of [33], which retains the orthogonality of codes even in delay-dispersive channels.

Figures 13 and 14 show the performance when two users (independent piconets) are operating simultaneously. The desired users are located at half the distance that gives the 90% outage probability (i.e., there is a 6 dB margin[6] with respect to the single-user case); shadowing is not considered in that graph. We find that an "interfering piconet" can be at a distance from the victim receiver of about 1 m (if the desired piconet is operating in CM1 or CM2) or 1.5 m (if the desired piconet is operating in CM3 or CM4). The performance does not depend on which channel model is used for the interfering piconet.

Table 1 shows the coexistence of our system with other communications devices, obeying various narrowband standards. In the column "desired," we list the interference power that must not be exceeded according to the specifications of the IEEE 802.15.3a technical requirements documentation (this power is derived from the receivers' sensitivity specifications for various systems). In the "achieved" column, we list the interference power (within the victim receiver bandwidth) received from our UWB transmitter spaced at 1 m distance from the victim receiver. The column "FCC mask" gives the interference power created by a UWB transmitter (at 1 m distance) that transmits at all frequencies with the maximum power allowed by the FCC mask. We find that if the UWB transmitter emits with the full power allowed by the FCC, it can significantly interfere with other communications devices. A suppression of about 15 dB is necessary to allow coexistence within a 1 m range. We achieve this suppression with the spectral shaping as described in Section 3.3.

[6] As the channel model prescribes the received power to be proportional to d^{-2}, halving the distance means increasing the power by 6 dB.

Finally, we also analyzed the resistance of the UWB system to interference *from* other communications devices. We found that again, a minimum distance of 1 m is sufficient to allow operation with less than 8% PER.

7. SUMMARY AND CONCLUSIONS

We have presented a UWB communications system based on TH-IR. This system uses only baseband components, while still being compatible with FCC requirements, and providing a flexible shaping of the transmit spectrum in order to accommodate future requirements by other spectrum governing agencies, as well as not to interfere with 802.11a wireless LANs and other communications receivers in the microwave range. Our system can sustain data rates of 110 Mbps at 15 m in AWGN channels, and 4–7 m in multipath channels. It is also resistant to interference from other UWB users, as well as interference from wireless LANs, microwave ovens, and other interferers.

APPENDIX

PARAMETER ESTIMATION

To obtain uniform samples, the timing of the lth finger corresponding to the mth training sequence is adjusted as follows:

$$t_{l,m} = 4(l-1)\Delta + (m-1)\Delta, \tag{A.1}$$

for $l = 1, \ldots, 10$, and $m = 1, \ldots, 4$.

Let the training sequence be b_k^t's for $k = 0, 1, \ldots, 510$, where superscript t denotes "training." Then the training signal can be expressed as

$$s^t(t) = \sum_{k=0}^{510} b_k^t w(t - kT_s). \tag{A.2}$$

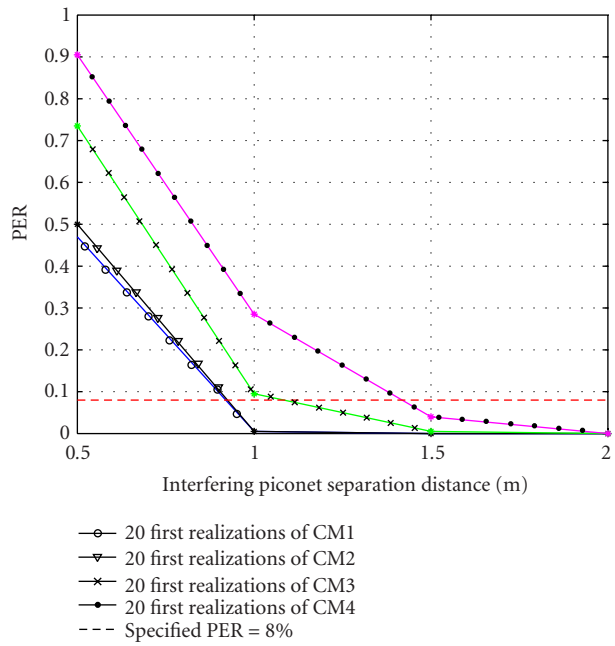

Figure 13: Packet error rate as a function of the distance of an interfering piconet from the receiver (normalized to the distance between the desired piconet transmitter to the receiver) in CM1.

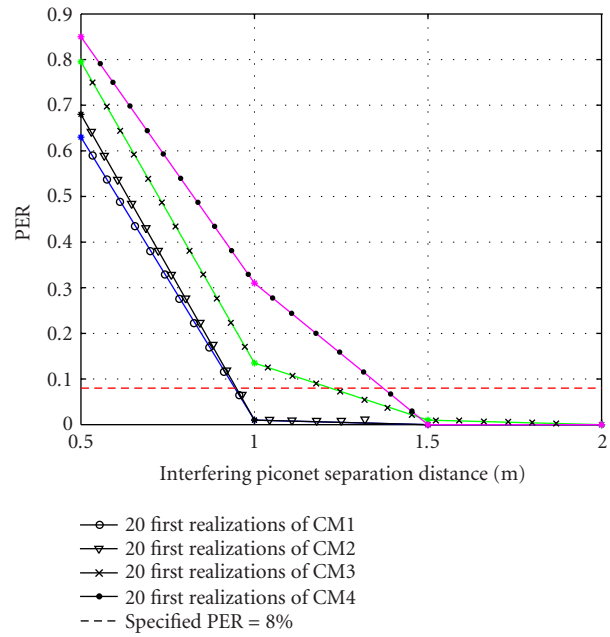

Figure 14: Packet error rate as a function of the distance of an interfering piconet in CM3.

From (15), the Δ-spaced output of the matched filter is

$$y^t(n\Delta) = \sum_{k=0}^{510} b_k^t \tilde{h}(n\Delta - kp\Delta) + \tilde{n}(n\Delta). \tag{A.3}$$

Consequently, the estimated channel taps can be expressed as

$$\tilde{h}(n\Delta) = \frac{1}{511} \sum_{k=0}^{510} b_k^t y^t(n\Delta + kp\Delta). \tag{A.4}$$

It can be shown that

$$\begin{aligned}\tilde{h}(n\Delta) = h(n\Delta) &+ \frac{1}{511} \sum_{m=0}^{510} \left(\sum_{k=m}^{510} b_k^t b_{k-m}^t \right) h(n\Delta + mp\Delta) \\ &+ \frac{1}{511} \sum_{m=-510}^{0} \left(\sum_{k=0}^{510-m} b_k^t b_{k-m}^t \right) h(n\Delta + mp\Delta) \\ &+ \frac{1}{511} \sum_{k=0}^{510} b_k^t \tilde{n}(n\Delta + kp\Delta).\end{aligned} \tag{A.5}$$

The second and third terms in the above equation are the perturbations from other taps due to imperfect orthogonality of the training sequence and the forth term presents the effect of channel noise.

To exploit the improved approach for UWB systems with cochannel interference, interference power has to be estimated. Using the estimated channel and the training sequence, the interference can be estimated by

$$i_t[n] = y_t(n\Delta) - \sum_{k=0}^{510} b_k^t \tilde{h}(n\Delta - kp\Delta), \tag{A.6}$$

and from it, interference-plus-noise power can be estimated by

$$P_k = \frac{1}{511} \sum_{m=0}^{510} |\, i_t[mp + k] \,|^2, \tag{A.7}$$

for $k = 0, 1, \ldots, (p-1)$.

Next, we determine the RAKE weights. Let $n_1, \ldots, n_L$ be the indices of the L largest taps. Then the weights for the MMSE RAKE combiner and optimum timing can be found by minimizing

$$\begin{aligned}\mathrm{MSE}\,(\vec{\gamma}, n_0) &= \frac{1}{511} \sum_{n=0}^{510} |\, z_t(n, n_0) - b_n^t \,|^2 \\ &= \frac{1}{511} \sum_{n=0}^{510} \left| \sum_{l=1}^{10} \gamma_l y_t(pn + n_l + n_0) - b_n^t \right|^2.\end{aligned} \tag{A.8}$$

Table 1: Coexistence for other systems.

System	Desired	Achieved	FCC mask
802.11a	−88 dBm	−90 dBm	−75 dBm
802.11b	−82 dBm	−85 dBm	−70 dBm
802.15.1	−76 dBm	−95 dBm	−80 dBm
802.15.3	−81 dBm	−85 dBm	−70 dBm
802.15.4	−91 dBm	−95 dBm	−80 dBm

Direct least-squares calculation yields that [34]

$$\vec{\gamma} = \begin{pmatrix} \gamma_1 \\ \vdots \\ \gamma_{10} \end{pmatrix} = \left(\mathbf{Y}_t \mathbf{Y}_t^{\mathrm{H}}\right)^{-1} \left(\mathbf{Y}_t \mathbf{b}_t^{\mathrm{H}}\right), \tag{A.9}$$

where

$$\mathbf{Y}_t = \begin{pmatrix} y_t[n_1 + n_o] & \cdots & y_t[510p + n_1 + n_o] \\ y_t[n_2 + n_o] & \cdots & y_t[510p + n_2 + n_o] \\ \vdots & \vdots & \vdots \\ y_t[n_{10} + n_o] & \cdots & y_t[510p + n_{10} + n_o] \end{pmatrix}, \tag{A.10}$$

$$\mathbf{b}_t = \begin{pmatrix} b_0^t & b_1^t & \cdots & b_{510}^t \end{pmatrix}.$$

From the estimated weights for the RAKE receiver, its output can be calculated by

$$z_t[n, n_o] = \sum_{l=1}^{10} \gamma_l y_t[pn + n_l + n_o]. \tag{A.11}$$

The equalizer coefficients can be estimated by minimizing

$$\frac{1}{511} \sum_{n=0}^{511} \left| \sum_{k=-L}^{L} c_k z_t[n-k, n_o] - b_k^t \right|^2. \tag{A.12}$$

Consequently [34],

$$\begin{pmatrix} c_{-2} \\ \vdots \\ c_2 \end{pmatrix} = \left(\frac{1}{511} \sum_{k=0}^{510} \mathbf{z}_k^t \left(\mathbf{z}_k^t\right)^{\mathrm{T}} \right)^{-1} \left(\frac{1}{511} \sum_{k=0}^{510} \mathbf{z}_k^t b_k^t \right), \tag{A.13}$$

where

$$\mathbf{z}_k^t = \begin{pmatrix} z_t[k+2, n_o] \\ \vdots \\ z_t[k-2, n_o] \end{pmatrix}. \tag{A.14}$$

ACKNOWLEDGMENT

Part of this work was presented at WPMC 2003, Yokosuta, Japan.

REFERENCES

[1] J. D. Taylor, Ed., *Introduction to Ultra-Wideband Radar Systems*, CRC Press, Boca Raton, Fla, USA, 1st edition, 1995.

[2] R. A. Scholtz, "Multiple access with time-hopping impulse modulation," in *Proc. IEEE Military Communications Conference (MILCOM '93)*, vol. 2, pp. 447–450, Boston, Mass, USA, October 1993.

[3] M. Z. Win and R. A. Scholtz, "Impulse radio: how it works," *IEEE Commun. Lett.*, vol. 2, no. 2, pp. 36–38, 1998.

[4] M. Z. Win and R. A. Scholtz, "Ultra-wide bandwidth time-hopping spread-spectrum impulse radio for wireless multiple-access communications," *IEEE Trans. Commun.*, vol. 48, no. 4, pp. 679–689, 2000.

[5] S. S. Kolenchery, J. K. Townsend, and J. A. Freebersyser, "A novel impulse radio network for tactical military wireless communications," in *Proc. IEEE Military Communications Conference (MILCOM '98)*, vol. 1, pp. 59–65, Boston, Mass, USA, October 1998.

[6] M. Ho, L. Taylor, and G. Aiello, "UWB technology for wireless video networking," in *Proc. International Conference on Consumer Electronics (ICCE '01)*, pp. 18–19, Los Angeles, Calif, USA, June 2001.

[7] C. J. Le Martret and G. B. Giannakis, "All-digital impulse radio for MUI/ISI-resilient multiuser communications over frequency-selective multipath channels," in *Proc. 21st Century Military Communications Conference (MILCOM '00)*, vol. 2, pp. 655–659, Los Angeles, Calif, USA, October 2000.

[8] J. Conroy, J. L. LoCicero, and D. R. Ucci, "Communication techniques using monopulse waveforms," in *Proc. IEEE Military Communications Conference (MILCOM '99)*, vol. 2, pp. 1181–1185, Atlantic City, NJ, USA, October–November 1999.

[9] A. R. Forouzan, M. Nasiri-Kenari, and J. A. Salehi, "Performance analysis of ultrawideband time-hopping code division multiple access systems: uncoded and coded schemes," in *Proc. IEEE International Conference on Communications (ICC '01)*, vol. 10, pp. 3017–3021, Helsinki, Finland, June 2001.

[10] D. Cassioli, M. Z. Win, F. Vatalaro, and A. F. Molisch, "Effects of spreading bandwidth on the performance of UWB RAKE receivers," in *Proc. IEEE International Conference on Communications (ICC '03)*, vol. 5, pp. 3545–3549, Anchorage, Alaska, USA, May 2003.

[11] E. Fishler and H. V. Poor, "On the tradeoff between two types of processing gain," in *Proc. 40th Annual Allerton Conference on Communication, Control, and Computing*, Monticello, Ill, USA, October 2002.

[12] Federal Communications Commission (FCC), *Revision of Part 15 of the Commission's Rules Regarding Ultra Wideband Transmission Systems*, First Report and Order, ET Docket 98-153, FCC 02-48; Adopted: February, 2002; Released: April, 2002.

[13] *IEEE Conference on Ultra wideband Systems and Technologies*, Baltimore, Md, USA, 2002.

[14] *International Workshop on Ultrawideband Systems*, Oulu, Finland, 2003.

[15] L. Zhao and A. Haimovich, "Performance of ultra-wideband communications in the presence of interference," *IEEE J. Select. Areas Commun.*, vol. 20, no. 9, pp. 1684–1691, 2002.

[16] F. Ramirez-Mireles, "Performance of ultrawideband SSMA using time hopping and M-ary PPM," *IEEE J. Select. Areas Commun.*, vol. 19, no. 6, pp. 1186–1196, 2001.

[17] M. Z. Win and R. A. Scholtz, "On the energy capture of ultrawide bandwidth signals in dense multipath environments," *IEEE Commun. Lett.*, vol. 2, no. 9, pp. 245–247, 1998.

[18] D. Cassioli, M. Z. Win, and A. F. Molisch, "The ultra-wide bandwidth indoor channel: from statistical model to simulations," *IEEE J. Select. Areas Commun.*, vol. 20, no. 6, pp. 1247–1257, 2002.

[19] A. Batra, J. Balakrishnan, A. Dabak, et al., "Multiband OFDM physical layer proposal," IEEE 802.15-03/267r2, 2003.

[20] J. McCorkle et al., "Xtremespectrum CPF document," IEEE 802.15-03/154r0, 2003.

[21] V. G. Subramanian and B. Hajek, "Broad-band fading channels: signal burstiness and capacity," *IEEE Trans. Inform. Theory*, vol. 48, no. 4, pp. 809–827, 2002.

[22] A. F. Molisch, M. Miyake, and J. Zhang, "Time hopping versus frequency hopping in ultrawideband systems," in *Proc. IEEE Pacific Rim Conference on Communications, Computers and signal Processing (PACRIM '03)*, vol. 2, pp. 541–544, Victoria, British Columbia, Canada, August 2003.

[23] Y. Wu, A. F. Molisch, S. Y. Kung, and J. Zhang, "Impulse radio pulse shaping for ultra-wide bandwidth (UWB) systems," in *Proc. 14th IEEE International Symposium on Personal, Indoor, and Mobile Radio Communications (PIMRC '03)*, vol. 1, pp. 877–881, Beijing, China, September 2003.

[24] Y. P. Nakache and A. F. Molisch, "Spectral shape of UWB signals—influence of modulation format, multiple access scheme and pulse shape," in *Proc. 57th IEEE Semiannual Vehicular Technology Conference (VTC '03)*, vol. 4, pp. 2510–2514, Jeju, South Korea, April 2003.

[25] S. Gezici, E. Fishler, H. Kobayashi, H. V. Poor, and A. F. Molisch, "A rapid acquisition technique for impulse radio," in *Proc. IEEE Pacific Rim Conference on Communications, Computers and signal Processing (PACRIM '03)*, vol. 2, pp. 627–630, Victoria, British Columbia, Canada, August 2003.

[26] H. Sheng, P. Orlik, A. M. Haimovich, L. Cimini, and J. Zhang, "On the spectral and power requirements for ultra-wideband transmission," in *Proc. IEEE International Conference on Communications (ICC '03)*, vol. 1, pp. 738–742, Anchorage, Alaska, USA, May 2003.

[27] N. Lehmann and A. M. Haimovich, "The power spectral density of a time hopping UWB signal: a survey," in *Proc. IEEE Conference on Ultra Wideband Systems and Technologies (UWBST '03)*, pp. 234–239, Reston, Va, USA, November 2003.

[28] N. Lehmann and A. M. Haimovich, "New approach to control the power spectral density of a time hopping UWB signal," in *Proc. 37th Conference on Information Sciences and Systems (CISS '03)*, Baltimore, Md, USA, March 2003.

[29] A. F. Molisch, J. R. Foerster, and M. Pendergrass, "Channel models for ultrawideband personal area networks," *IEEE Personal Comm. Mag.*, vol. 10, no. 6, pp. 14–21, 2003.

[30] D. Cassioli, M. Z. Win, F. Vatalaro, and A. F. Molisch, "Performance of low-complexity RAKE reception in a realistic UWB channel," in *Proc. IEEE International Conference on Communications (ICC '02)*, vol. 2, pp. 763–767, New York, NY, USA, April–May 2002.

[31] J. D. Choi and W. E. Stark, "Performance of ultra-wideband communications with suboptimal receivers in multipath channels," *IEEE J. Select. Areas Commun.*, vol. 20, no. 9, pp. 1754–1766, 2002.

[32] D. C. Cox, "Delay doppler characteristics of multipath propagation at 910 MHz in a suburban mobile radio environment," *IEEE Trans. Antennas Propagat.*, vol. 20, no. 5, pp. 625–635, 1972.

[33] L. Yang and G. B. Giannakis, "Impulse radio multiple access through ISI channels with multi-stage block-spreading," in *Proc. IEEE Conference on Ultra Wideband Systems and Technologies (UWBST '02)*, pp. 277–281, Baltimore, Md, USA, May 2002.

[34] S. Haykin, *Adaptive Filter Theory*, Prentice Hall, Upper Saddle River, NJ, USA, 3rd edition, 1996.

Andreas F. Molisch received the Dipl.-Ing. and Dr. Tech. degrees from the Technical University Vienna, Austria, in 1990 and 1994, respectively. From 1991 to 2000, he was with the TU Vienna, and from 2000 to 2002, he was with AT&T Laboratories Research. Since then, he has been a Senior Principal Member of Technical Staff with Mitsubishi Electric Research Laboratories, Cambridge, Mass. He is also a Professor and Chairholder for radio systems at Lund University, Sweden. Dr. Molisch's current research interests are in MIMO systems, measurement and modeling of mobile radio channels, and ultra-wideband (UWB). He has authored, coauthored, or edited two books, eight book chapters, some 85 journal papers, and numerous conference contributions. He is an Editor of the IEEE Transactions on Wireless Communications, Coeditor of an upcoming special issue of IEEE JSAC on UWB, and Vice-Chair of the TPC of the IEEE Vehicular Technology Conference, spring 2005. He is the Chairman of the COST273 and IEEE 802.15.4a Channel Modeling Groups and Vice-Chairman of Commission C of URSI (International Union of Radio Scientists). Dr. Molisch is a Fellow of the IEEE and a recipient of several awards.

Ye Geoffrey Li received his B.S.E. and M.S.E. degrees in 1983 and 1986, respectively, from the Department of Wireless Engineering, Nanjing Institute of Technology, Nanjing, China, and his Ph.D. degree in 1994 from the Department of Electrical Engineering, Auburn University, Alabama. After spending several years at AT&T Labs-Research, he joined the School of Electrical and Computer Engineering, Georgia Tech, as an Associate Professor in 2000. His general research interests include statistical signal processing and wireless communications. In these areas, he has contributed over 100 papers published in referred journals and presented in various international conferences. He also has over 10 US patents, granted or pending. He once served as a Guest Editor for two special issues on signal processing for wireless communications for the IEEE JSAC and an Editorial Board Member of EURASIP Journal on Applied Signal Processing. He is currently serving as an Editor for wireless communication theory for the IEEE Transactions on Communications. He organized and chaired many international conferences, including Technical Program Vice-Chair of IEEE 2003 International Conference on Communications.

Yves-Paul Nakache was born in Longjumeau, France, on December 20, 1976. He received the M.S. degree with high honors from the École Superieure d'Ingenieurs en Electronique et Electrotechnique de Paris (ESIEE Paris) in 2000, as well as the Price of Excellence from NEC Electronics, France. He received his B.S. degree in physics, concurrently, from the University Paris VII in 1998. While he was a student, his research activity focused on a very low-bit encoding of prosody for a speech vocoder with Thomson-CSF Communication (now Thales Communication) for the RNRT Project SYMPATEX. In 2000, he joined Mitsubishi Electric Research Laboratories. His current research interests include spectral shaping for impulse radio ultra-wideband (UWB) transceivers, spreading techniques for multiband OFDM systems, and low-complexity UWB transceivers with compatibility to multiband OFDM.

Philip Orlik was born in New York, NY, in 1972. He received the B.E. degree in 1994 and the M.S. degree in 1997, both from the State University of New York (SUNY), Stony Brook. In 1999, he received his Ph.D. degree in electrical engineering also from SUNY Stony Brook. He is currently a Principal Technical Staff Member at Mitsubishi Electric Research Laboratories Inc. located in Cambridge, Mass.

His primary research focuses is on sensor networks, ad hoc networking, and ultra-wideband (UWB). Other research interests include mobile cellular and wireless communications, mobility modeling, performance analysis, queueing theory, and analytical modeling

Makoto Miyake received the B.S. and M.S. degrees in electronics engineering from Kobe University, Hyogo, Japan, in 1973 and 1975, respectively, and the Dr. Eng. degree in communication engineering from Osaka University, Osaka, Japan, in 1990. He has been with Mitsubishi Electric Corporation since 1975, where he has been engaged in research and development of digital communication technologies of modulation/demodulation, spread-spectrum signaling, forward-error correction coding, diversity, and synchronization. He conducted the design and development of digital wireless communication systems, including the INTELSAT TDMA satellite communication systems, mobile-satellite communication systems, the personal digital cellular (PDC), the personal handy phone system (PHS), the wideband code-division multiple-access (W-CDMA) system, and the intelligent transport systems (ITS). From 1996 to 1999, he participated in a European R&D programme of the Advanced Communication Technologies and Services (ACTS), and conducted the development of a broadband wireless receiver incorporating a high-speed Viterbi equalizer for mobile broadband systems. He is currently a Chief Engineer in the Information Technology R&D Center, Mitsubishi Electric Corporation. Dr. Miyake is an IEEE Fellow, a Member of the IEICE Japan, and a Member of the Society of Information Theory and Its Application of Japan.

Yunnan Wu received the B.E. degree in computer science from University of Science and Technology of China, Hefei, in 2000, and the M.A. degree in electrical engineering from Princeton University in 2002. He is currently pursuing his Ph.D. degree with the Department of Electrical Engineering, Princeton University. He was with Microsoft Research Asia, Beijing, China, from 1999 to 2001, as a Research Assistant, with Bell Laboratories, Lucent Technologies, Murray Hill, NJ, as a Summer Intern in 2002, and with Microsoft Research, Redmond, Wash, as a Summer Intern in 2003. His research interests include networking, wireless communications, signal processing, information theory, and multimedia. Mr. Wu received the Best Student Paper Award at the 2000 SPIE and IS&T Visual Communication and Image Processing Conference. He is a recipient of Microsoft Research Graduate Fellowship for 2003–2004.

Sinan Gezici was born in 1979. He received the B.S. degree from Bilkent University, Turkey, in 2001, and the M.A. degree from Princeton University in 2003. He is currently working toward the Ph.D. degree at the Department of Electrical Engineering, Princeton University. His main fields of interest are in wireless geolocation and ultra-wideband (UWB) communications.

Harry Sheng received the B.S. and M.S. degrees in electrical engineering from Xidian University, Xi'an, China, in 1992 and 1995, respectively. He is currently working toward the Ph.D. degree at the Department of Electrical and Computer Engineering, New Jersey Institute of Technology, Newark, NJ, USA. His research interests include communications and signal processing, in particular, the pulse waveform design, optimum combining and interference cancellation, synchronization, and channel estimation for ultra-wideband (UWB) communications.

S. Y. Kung received his Ph.D. degree in electrical engineering from Stanford University. Since 1987, he has been a Professor of electrical engineering at the Princeton University. His research interests include wireless communication, sensor-array processing, spectrum analysis, image processing and recognition, neural networks, signal processing, VLSI array processors, system modeling and identification, multimedia signal processing, and bioinformatic information processing. Professor Kung has authored more than 300 technical publications and numerous text and reference books. Since 1990, he has served as an Editor-In-Chief of Journal of VLSI Signal Processing Systems. He was a Founding Member of IEEE Signal Processing Society's Technical Committees on VLSI Signal Processing, Machine Learning for Signal Processing, and Multimedia Signal Processing. Professor Kung has been a Fellow of IEEE since 1988. He was the recipient of IEEE Signal Processing Society's Technical Achievement Award in 1992 for his contributions on "parallel processing and neural network algorithms for signal processing;" an IEEE-Signal Processing Society's Distinguished Lecturer in 1994; a recipient of the 1996 IEEE Signal Processing Society's Best Paper Award for his work on principal component neural networks; and a recipient of the IEEE Third Millennium Medal in 2000.

H. Kobayashi is the Sherman Fairchild University Professor of electrical engineering and computer science at Princeton University since 1986, when he joined the Princeton faculty as the Dean of the School of Engineering and Applied Science (1986–1991). From 1967 till 1982, he was with the IBM Research Center, Yorktown Heights, and from 1982 to 1986, he served as the Founding Director of the IBM Tokyo Research Laboratory. His research experiences include radar systems, high-speed data transmission, coding for high-density digital recording, image compression algorithms, performance modeling, and analysis of computers and communication systems. His current research activities are in performance modeling and analysis of high-speed networks, wireless communications and geolocation algorithms, network security, and teletraffic and queuing theory. He has authored more than 150 research articles, and has published a textbook *Modeling and Analysis* (Addison-Wesley, 1978). He is a Member of the Engineering Academy of Japan and a Life Fellow of IEEE. He was the recipient of the Humboldt Prize from Germany (1979), the IFIP Silver Core Award (1981), and two IBM Outstanding Contribution Awards. He received his Ph.D. degree in 1967 from Princeton University and the B.E. and M.E. degrees in 1961 and 1963 from the University of Tokyo, all in electrical engineering.

H. Vincent Poor received the Ph.D. degree in EECS from Princeton University, in 1977. From 1977 till 1990, he was on the faculty of the University of Illinois at Urbana-Champaign. Since 1990, he has been on the faculty at Princeton University, where he is the George Van Ness Lothrop Professor in engineering. He has also held visiting appointments at a number of universities, including recently Imperial College, Stanford, and Harvard. Dr. Poor's research interests are in the areas of advanced signal processing, wireless networks, and related fields. Among his publications in these areas is the recent book, *Wireless Networks: Multiuser Detection in Cross-Layer Design* (Springer, 2005). Dr. Poor is a Member of the National Academy of Engineering and is a Fellow of the IEEE, the Institute of Mathematical Statistics, the Optical Society of America, and other organizations. He is a past President of the IEEE Information Theory Society, and is the current Editor-in-Chief of the IEEE Transactions on Information Theory. Recent recognition of his work includes the Joint Paper Award of the IEEE Communications and Information Theory Societies (2001), the NSF Director's Award for Distinguished Teaching Scholars (2002), a Guggenheim Fellowship (2002–2003), and the IEEE Education Medal (2005).

Alexander Haimovich is a Professor of electrical and computer engineering at the New Jersey Institute of Technology (NJIT). He recently served as the Director of the New Jersey Center for Wireless Telecommunications, a state-funded consortium consisting of NJIT, Princeton University, Rutgers University, and Stevens Institute of Technology. He has been at NJIT since 1992. Prior to that, he served as a Chief Scientist of JJM systems from 1990 until 1992. From 1983 until 1990, he worked in a variety of capacities, up to Senior Staff Consultant, for AEL Industries. He received the Ph.D. degree in systems from the University of Pennsylvania in 1989, the M.S. degree in electrical engineering from Drexel University in 1983, and the B.S. degree in electrical engineering from the Technion, Haifa, Israel, in 1977. His research interests include MIMO systems, array processing for wireless, turbo-coding, space-time coding, ultra-wideband (UWB) systems, and radar. He recently served as a Chair of the Communication Theory Symposium at Globecom 2003. He is currently an Associate Editor for the IEEE Communications Letters and a Guest Editor for the EURASIP Journal on Applied Signal Processing's special issue on turbo coding.

Jinyun Zhang received her Ph.D. degree in electrical engineering from the University of Ottawa in 1991. She is currently a Senior Principal Technical Staff and a Group Manager of Digital Communication and Networking Group at Mitsubishi Electric Research Laboratories (MERL). She currently manages various wireless communications and networking projects that include ultra-wideband (UWB), IEEE802.11WLAN, ZigBee, sensor network, and 3G/4G wireless communications. Prior to joining MERL, she worked for Nortel Networks for more than 10 years, where she held engineering and management positions in the areas of VLSI design, advanced wireless technology development, and wireless and optical networks.